Excitation cross sections of Cd+ ions for the upper and lower states of the Cd II 441.6-nm laser line by electron impact

doi: 10.1103/PhysRevA.27.124

Excitation cross sections of Cd^+ ions for the upper and lower states of the Cd II 441.6-nm laser line by electron impact

K. Hane, T. Goto, and S. Hattori
Department of Electronics, Faculty of Engineering, Nagoya University, Nagoya 464, Japan
(Received 13 April 1982)

The excitation cross sections by electron impact from the Cd II ground state to the laser upper state $5s^2\,^2D_{5/2}$ (Beutler state) and the laser lower state $5p\,^2P_{3/2}$ (resonance state) have been measured by using a crossed-beam method of electrons and Cd^+ ions and a photon-counting method. The electron-energy region investigated was from the threshold energy (5.8 eV) for the excitation of the $5p\,^2P_{3/2}$ state to 20 eV. It has been shown that the excitation cross section for the ionic Beutler state $5s^2\,^2D_{5/2}$ is of the order of 10^{-15} cm^2 and has a sharp peak near the threshold energy for the excitation. The excitation cross section for the resonance state $5p\,^2P_{3/2}$ has also been of the order of 10^{-15} cm^2 and has a relatively broad maximum.

I. INTRODUCTION

One of the most stable and useful metal ion lasers is the positive column He-Cd^+ laser (441.6 nm). As the dominant excitation process for the upper state $5s^2\,^2D_{5/2}$ of the 441.6-nm laser, the following stepwise excitation process (1) was proposed[1]:

$$\begin{aligned} &Cd+e\rightarrow Cd^+ +2e\ , \\ &Cd^+ +e\rightarrow Cd^+(5s^2\,^2D_{5/2})+e\ , \end{aligned} \tag{1}$$

where Cd are atoms in the neutral ground state and Cd^+ are ions in the Cd II ground state. Subsequently, several results have been reported which support it.[2–4] At the present stage, it is desired to determine the excitation cross section $\sigma(5s^2\,^2D_{5/2})$ for the process

$$Cd^+ +e\rightarrow Cd^+(5s^2\,^2D_{5/2})+e\ ,$$

and moreover, the excitation cross section $\sigma(5p\,^2P_{3/2})$ for the process

$$Cd^+ +e\rightarrow Cd^+(5p\,^2P_{3/2})+e$$

by which the laser lower state $5p\,^2P_{3/2}$ is populated. An energy level diagram of Cd II including those states is shown in Fig. 1.

The measurements of the excitation cross sections of metallic ions by electron impact have been limited to the resonance states of Zn II,[5] Hg II,[6] Ca II,[7,8] Ba II,[8–10] Mg II,[8] and Sr II (Ref. 8) and very few higher excited states of them.[5,8,10,11] On the other hand, as to the Cd^+ ions, only the ratio

$$\sigma(5s^2\,^2D_{5/2})/\sigma(5p\,^2P_{3/2})$$

at a 13-eV electron energy has been measured.[12] However, for any excited state of Cd II, the absolute value and energy dependence of the excitation cross section from the Cd II ground state by electron impact have not been reported up to the present. Particularly, the Cd II $5s^2\,^2D_{5/2}$ state is called the Beutler state in which one of the inner-shell electrons is excited. The cross-section measurement for the excitation of a bound state of an ion by promotion of an inner-shell electron is a subject of some general current interest. The absolute cross section from the ionic ground state to the ionic Beutler state has never been investigated for any metal experimentally.

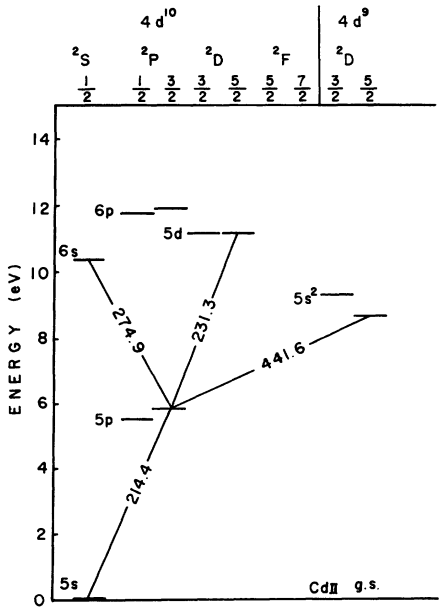

FIG. 1. Energy level diagram of Cd II.

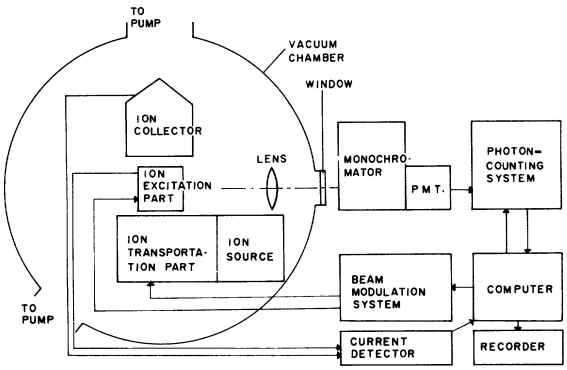

FIG. 2. Block diagram of the experimental apparatus.

In this work, the absolute values of $\sigma(5s^2\,{}^2D_{5/2})$ for the ionic Beutler state and $\sigma(5p\,{}^2P_{3/2})$ for the resonance state have been first measured in the region of the threshold energy for the excitation to 20 eV, by using a crossed-beam method of electrons and Cd^+ ions and a photon-counting technique.

II. EXPERIMENTAL TECHNIQUES AND APPARATUS

A. General

Figure 2 shows the schematic diagram of the experimental apparatus. A crossed-beam apparatus consisting of an ion source, an ion transportation part, an excitation part of Cd^+ ions, and an ion collector is placed in a vacuum chamber of 450-mm diameter. The vacuum chamber is pumped by two oil diffusion pumps of 4 in. and 3 in. and is evacuated to a pressure of 10^{-8} Torr. A collimated ion beam is crossed at a right angle by an electron beam at the excitation part of Cd^+ ions. The ions are excited to various states by electron impact and then emit photons, which are observed in a cone along the third orthogonal axis by the detection apparatus. The detection apparatus consists of a quartz lens, a vacuum chamber window, a monochromator, a photomultiplier tube, and a photon-counting system. In order to separate a photon count rate into the signal and the background noise, both the ion and electron beams are modulated. The photon-counting system and the beam modulation system are controlled by a minicomputer.

The absolute emission cross section of the spectral line is obtained from the following equation[9]:

$$\sigma_{em}=(1-\tfrac{1}{3}P)\frac{S}{I_iI_e}\frac{e^2v_iv_e}{(v_i^2+v_e^2)^{1/2}}\frac{F}{D}\,, \tag{2}$$

where P represents the polarization fraction of photons collected, S is the recorded count rate of photons, I_i is the total ion beam current, I_e is the total electron beam current, v_i is the ion velocity, v_e is the electron velocity, e is the electric charge, F is the form factor,[9] and D is the absolute sensitivity for the detection system of photons at the wavelength concerned.

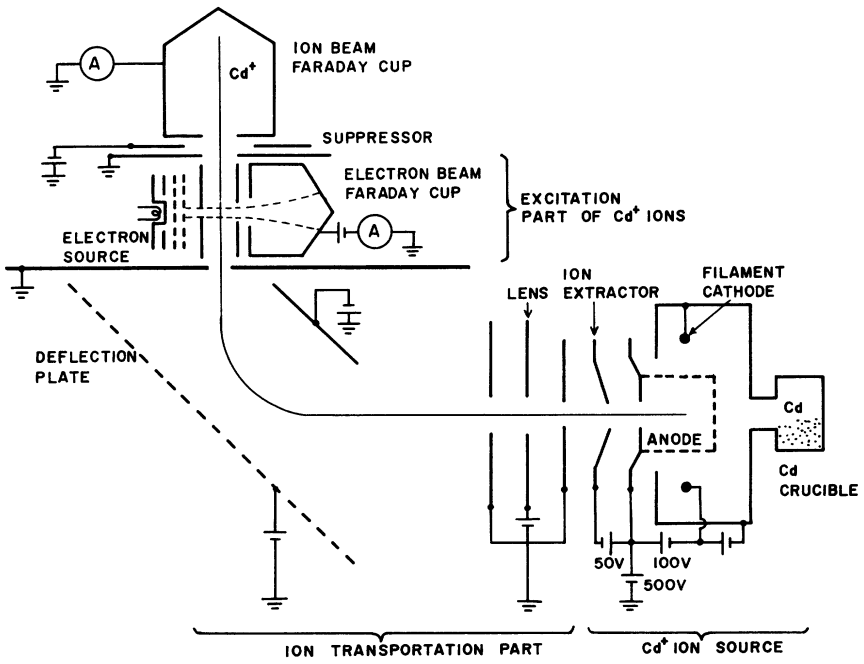

FIG. 3. Schematic diagram of the crossed-beam apparatus viewed from above but with the electron beam rotated by 90° from a vertical to horizontal position in order to represent its parts.

B. Crossed-beam apparatus

Figure 3 shows the schematic diagram of the crossed-beam apparatus. An ion source used for this experiment is the electron bombardment ion source, which was developed for the gas ion source by Khan.[13] It was modified and used as a metal ion source. The cylindrical mesh anode is placed so that its axis could coincide with the ion beam axis. The circular filament cathode made of thoriated tungsten wire of 0.2-mm diameter encircles coaxially the cylindrical mesh anode. Furthermore, the ion source is enclosed by the stainless cylinder. Electrons emitted from the filament cathode are accelerated toward the anode. Although some of them ionize Cd atoms in the anode cage, many of them pass through the mesh of the anode to go forward to the wall of the stainless cylinder. However, since the stainless cylinder is kept at the same potential as the filament cathode, those electrons are moved backward to the mesh of the anode and pass through it. This motion is repeated several times until they are finally collected by the anode. This results in a rather increased flux density of Cd^+ ions. The ions produced by electron-atom collisions inside the anode cage are extracted by an extracting plate maintained at 50 V negative with respect to the anode.

The temperature of the Cd crucible was about 150 °C and the estimated Cd vapor pressure in the ion source was about 10^{-5} Torr. The heating current of the filament cathode was 3 to 4 A. The filament cathode was maintained at about 100 V negative with respect to the anode. The electron emission current of the filament cathode was 20 to 40 mA. The obtained ion current increased with the electron emission current and the Cd atom density.

The ions extracted from the ion source are accelerated and transported in the transportation part. Since the potential of the anode cage of the ion source is maintained at 500 V positive with respect to the ground, the extracted ions are accelerated up to about 500 V between the anode aperture and the first aperture of the Einzel lens. The accelerated ions are collimated by the Einzel lens and transported to the deflection region. The ions are deflected by the two deflection plates. Those deflection plates are used for pulsing of the ion beam. The deflected ion beam passes through the slit of 6-mm width by 4-mm height and then enters into the excitation part of Cd^+ ions designed to produce a field-free space, where the ion beam is crossed at a right angle by the electron beam. The ion beam emerging from the excitation part of Cd^+ ions is collected by the Faraday cup. The collected ion current was 1 to 2 μA in the present experiment.

Since the energy of the bombarding electrons in the ion source was 100 eV, which was much higher than the multiple ionization potential of Cd, the multiply ionized ions were included in the ions formed in the ion source. The quantity of the Cd^+ ion current I_i was obtained by dividing the total ion current collected by the Faraday cup into the ratio of the single ionization cross section of Cd to sum of the multiple ones of Cd at an electron energy of 100 eV, because in our ion source most multiply charged Cd ions were estimated to be due to a single collision between electron and Cd atom. That ratio of the ionization cross sections of Cd was obtained by combining data in Refs. 14 and 15. The estimated Cd^+ ion current was about 80% of the total ion current collected by the Faraday cup.

When the ion source was operated without Cd metal in the crucible, the ion beam current was a few percent of the ion beam current with Cd metal in the crucible. Then, the ion current by the residual gas was supposed to be a few percent of the total ion beam current.

The purity of the Cd grains in the crucible was 99.999% and the measurement of the excitation cross sections was performed after degassing the Cd grains. Therefore the ion current due to the impurity gases coming out of the Cd grains was negligibly small.

An electron source has an oxide cathode and three grids: focusing aperture electrode, accelerating grid, and beam control grid. The extracted electron beam is limited by the aperture of 2-mm diameter and crosses the ion beam at a right angle in the excitation part of Cd^+ ions. The typical electron current collected by the Faraday cup was 5 to 30 μA at the acceleration potential of 6 to 20 V.

The electron beam of 2-mm diameter crossed the ion beam of 6-mm width and 4-mm height in the excitation part of Cd^+ ions. Then, the collision volume was the cylindrical shape of about 2-mm diameter and 4-mm length. Assuming that the ion beam in the excitation part was uniform, the form factor F was calculated according to the definition of Pace and Hooper.[9] The value of F used in Eq. (2) was 6 mm, which was equal to the ion beam width.

C. Photon detection and its sensitivity

The lens of 43-mm diameter and 102-mm focal length was placed at a distance of 178 mm from the center of the collision volume and focused the image of the collision volume on the entrance slit of the monochromator. The monochromator was Nikon G-250 model with a dispersion of 3 nm/mm on the exit slit plane. The slit of it was of 1-mm width and 10-mm height. The output of the photomultiplier

tube was processed for counting. Since the photomultiplier tube was manufactured for a photon-counting process, the background noise by the photomultiplier tube was a few counts per second without cooling.

The polarization fraction P for the 441.6-nm line was measured by using a polarizing film placed in front of the entrance slit of the monochromator. First, the axis of the polarizer was placed parallel to the electron beam and the count rate $S_{||}$ of the 441.6-nm photons was measured. Then the axis of the polarizer was placed perpendicular to the electron beam and the count rate $S_{\perp}$ was measured. The polarization fraction was obtained by[9]

$$P=(S_{||}-S_{\perp})/(S_{||}+S_{\perp}) .$$

In order to determine the absolute emission cross section of the spectral line, the absolute value of D in Eq. (2) must be determined for the wavelength concerned. The determination of D contained four procedures: (1) the calibration of the relative sensitivity of the optical detection system with wavelength, (2) the calibration of the secondary standard lamp, (3) the calibration of the absolute sensitivity of the optical detection system by using the secondary standard lamp, and (4) the calibration of the ion traveling effect.

(1) The relative variation of D with the wavelength was measured carefully and repeatedly by using the Electro Optics Associates model L-101 tungsten standard lamp and a deuterium lamp in the wavelength region of 300 to 600 nm and 200 to 400 nm, respectively. In the measurement, the standard lamp was placed at the position of the collision volume in the chamber and the output of the photomultiplier tube operated by dc mode was recorded changing the wavelength selected by the monochromator. The intensity of the tungsten standard lamp changed from 0.1 to 7 in the arbitrary units in the wavelength region of 300 to 700 nm. Then, it decreased with increasing the wavelength after reaching a maximum 8 at 900 nm. The detectable wavelength region of the photomultiplier tube was less than 700 nm. Considering the above and the data as to the stray light of the monochromator, the uncertainties of the calibration caused by the stray light due to the infrared light of the tungsten lamp was estimated to be 1% or less at 442- and 560-nm wavelengths. On the other hand, at a 214-nm wavelength, the uncertainty of the calibration caused by the stray light of the monochromator due to the visible light was negligible since the intensity of the deuterium lamp decreased smoothly with the increase of the wavelength. In the region of 300 to 400 nm, the calibrations by using the two lamps agreed well with each other. The uncertainties caused by this calibration procedure were evaluated to be about ± 15 and $\pm 5\%$ for the 214.4- and 441.6-nm wavelengths, respectively.

(2) Since the intensity of the tungsten lamp or the deuterium lamp was too high to compare directly with that of the signal of electron-ion collisions, the light emitting diode (Toshiba Electric Co., Ltd., model TLG-103) with a weak intensity was used as the secondary standard lamp.

The calibration of the absolute intensity of the secondary standard lamp was carried out at a different dark room. The tungsten standard lamp, the secondary standard lamp, a monochromator, and a photomultiplier tube were aligned and the intensities of the two lamps were compared directly at a 560-nm wavelength by measuring the output signal of the lock-in amplifier. Since the intensity of the tungsten standard lamp was higher by orders of magnitude than that of the secondary standard lamp, the tungsten standard lamp was placed far from the monochromator (~ 5 m) to reduce the intensity low enough compared with that of the secondary standard lamp. The efficiency of the monochromator to detect the light emitted at the different distances from the entrance slit of the monochromator was corrected by another lamp with the intermediate intensity, which was moved along the axis of the monochromator. It was obtained from those measurements that the 560-nm light intensity of the secondary standard lamp was smaller than that of the tungsten standard lamp by a factor of 2.0×10^6 and the absolute emission intensity of the secondary standard lamp was 7.6×10^9 photons/(sec sr nm) at 1-mA current and 560-nm wavelength. The influence of the stray light of the monochromator on this calibration procedure was negligible. The uncertainty due to the standard lamp intensity and the above transfer procedures was estimated to be about $\pm 10\%$.

(3) The secondary standard lamp was placed at the position of the collision volume in the chamber with the same geometrical and detection system as used to detect the signal of the electron-ion collisions. Then the calibration of the absolute sensitivity of the detection system was carried out at the wavelength of 560 nm by using the photon-counting method. The uncertainty due to the above calibration procedure was evaluated to be about $\pm 5\%$.

(4) The $5s^2\,^2D_{5/2}$ state has a long lifetime of about 0.8 μsec.[16] The ions formed in the ion source were accelerated by the voltage of 500 V and entered the excitation part of Cd^+ ions. Then, they passed through the excitation part in the time of 1.6 μsec. Therefore some of the ions excited to the $5s^2\,^2D_{5/2}$ state by electron-ion collisions left the excitation

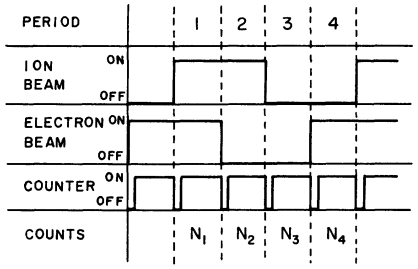

FIG. 4. Schematic diagram of the beam modulation sequence. N_1 contains the signal S, the noise N_i in phase with the ion beam, the noise N_e in phase with the electron beam, and the background noise N_b. N_2 contains N_i and N_b. N_3 contains N_b. N_4 contains N_e and N_b.

part of Cd^+ ions before they emitted the 441.6-nm photons and could not be observed by our optical detection system. The fraction of the ions emitting the 441.6-nm photons which could be observed by our optical detection system was calculated by ray tracing and was estimated to be 8.3% of the total ions excited to the $5s^2{}^2D_{5/2}$ state under the present experimental condition. This fraction was included in obtaining the absolute value of D in Eq. (2). The fraction (8.3%) of the total excitation rate for the $5s^2{}^2D_{5/2}$ state was equal to the cascading rate from the $5s^2{}^2D_{5/2}$ state to the $5p\,^2P_{3/2}$ state in the collision volume.

In the case of the 214.4-nm line, since the lifetime of the upper state is very short (3 nsec),[16] almost all of the ions excited to the $5p\,^2P_{3/2}$ state emitted the 214.4-nm photons in the collision volume and could be observed by our detection system.

After taking the above into account, the obtained values of D were 1.4×10^{-6} and 2.3×10^{-6} for the 441.6- and 214.4-nm lines, respectively. Combining the individual uncertainties in quadrature,[7,9] the total uncertainties of the above calibration procedures were evaluated to be $\pm12\%$ and $\pm20\%$ for the 441.6- and 214.4-nm wavelengths, respectively.

D. Data analysis

The output pulses from the photomultiplier tube were fed into the photon-counting system, which consisted of a preamplifier, a pulse shaper, and a binary counter. Since the noises caused by the ion and electron beams were larger in magnitude than the signal, the double-beam modulation was used for extracting the signal from the noise. Figure 4 shows the schematic diagram of the beam modulation sequence. There are four different periods as shown in Fig. 4. The time of each period used in the present experiment was 100 msec. The opening and closing of the gates of the counter and the beam modulation system were performed by the pulses from the timer which was included in the computer. There was a 4-msec time delay between ion (electron) beam switching and counter switching. The counter and the beam modulation system were controlled by the computer. The obtained counts per unit period were stored in the memory of the computer.

The symbols N_1, N_2, N_3, and N_4 are the count rates accumulated in the periods 1, 2, 3, and 4, respectively. The count rate S corresponding to the signal is derived from the equation

$$S=N_1-N_2+N_3-N_4\ .$$

The noise count rate N_i in phase with the ion beam is derived from $N_i=N_2-N_3$. The noise count rate N_e in phase with the electron beam is derived from $N_e=N_4-N_3$. The background noise count rate N_b is equal to N_3. The typical S was about 1 sec^{-1} and N_i, N_e, and N_b were about 200, 3, and 30 sec^{-1}, respectively, for the 411.6-nm line at the electron acceleration potential of 13 eV. For the 214.4-nm line, S was about 2 sec^{-1}. N_i, N_e, and N_b were about 50, 4, and 2 sec^{-1}, respectively, at the acceleration potential of 13 eV. The count $S_t(=ST)$ is the signal count accumulated in the measuring time T. The count S_t was accumulated until the standard deviation $(N_t)^{1/2}$ due to the Poisson statistics[9] of the total noise count N_t $[N_t=(N_i+N_e+N_b)T]$ was reduced to less than 15% of the count S_t.

Several consistency checks were carried out to confirm the proper operation of the apparatus. The S_t for the 441.6- and 214.4-nm wavelengths increased linearly with the time T, not at other wavelengths. Also the count S was proportional to the ion beam current and the electron beam current. Thus it was confirmed that the count rate S for the 441.6- and 214.4-nm wavelengths was the signals resulting from the electron-ion collisions.

When the acceleration potential of the electron beam was higher than the threshold energy of the direct excitation of Cd atoms for the Cd II $5s^2{}^2D_{5/2}$ state, N_e increased due to the direct excitation of Cd atoms escaping from the ion source. Then, it took a longer time to separate the signal from the noise. Here, the measurement was carried out in the low electron-energy region between the threshold energy and 20 eV.

III. RESULTS AND DISCUSSION

A. 214.4-nm line

Figure 5 shows the absolute emission cross section of the 214.4-nm line. The uncertainty of the mea-

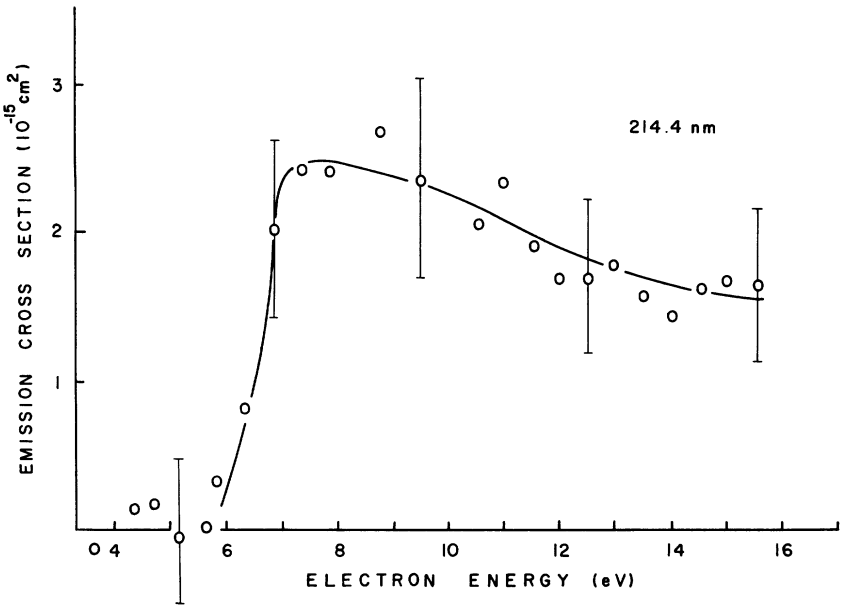

FIG. 5. Absolute emission cross section for the Cd II 214.4-nm line.

sured signal count (S_t) mainly depended on the statistical fluctuation of the total noise count N_t. We took $2(N_t)^{1/2}$ for the uncertainty of S_t, where $2(N_t)^{1/2}$ is twice the standard deviation of the total noise count N_t. The $2(N_t)^{1/2}$ was about 20% of the measured S_t. In addition to the uncertainty of S_t, the emission cross section included the uncertainty being caused by the measured ion and electron beam currents and the calibration of the sensitivity of the optical detection system. It was estimated to be about $\pm 25\%$. The total uncertainty was obtained by combining those uncertainties in quadrature[7,9] and was about $\pm 30\%$. The uncertainty was somewhat larger around threshold energy because of the small signal count rate. No attempt is made to include uncertainties in the estimated form factor, the correction for ion beam purity, or the radiation lifetime corrections; however, these uncertainties are believed to be small in comparison to those statistics and optical calibration which are given.

The measured emission cross section rises sharply at the threshold energy and changes slowly with the increase of the electron energy. This is similar to that of the emission cross section for the resonance line of Zn II.[5]

In the case of the 214.4-nm line, there are several cascading lines from the higher states to its upper state $5p\,^2P_{3/2}$. However, briefly examining several cascading lines under our experimental condition, the cascading rate from the higher states other than the $5s^2\,^2D_{5/2}$ state was negligible compared with that from the $5s^2\,^2D_{5/2}$ state. The cascading rate from the $5s^2\,^2D_{5/2}$ state could be evaluated using the measured photon count rate of the 441.6-nm line. Only less than 10% of the total excitation rate of the $5s^2\,^2D_{5/2}$ state cascaded to the $5p\,^2P_{3/2}$ state as described in Sec. II C. Then, the cascading rate to the $5p\,^2P_{3/2}$ state was about 20% of the total excitation rate of the $5p\,^2P_{3/2}$ state at most. The absolute cross section $\sigma(5p\,^2P_{3/2})$ for the $5p\,^2P_{3/2}$ state obtained after the subtraction of the cascading rate from the $5s^2\,^2D_{5/2}$ state is of the order of 10^{-15} cm^2.

There has been no report about the quantum-mechanical calculation of the excitation cross sections from the Cd II ground state to the Cd II excited states. However, Mewe[17] obtained the semiempirical formula. Using the optical oscillator strength (0.39) for the Cd II 214.4-nm line,[18] the value of $\sigma(5p\,^2P_{3/2})$ calculated by Mewe's formula was 1.7×10^{-15} cm^2 at the threshold energy, while the measured value of $\sigma(5p\,^2P_{3/2})$ was 2.3×10^{-15} cm^2.

The value of $\sigma(5p\,^2P_{3/2})$ measured here is larger by a factor of about 3 than that of the electron excitation cross section from the Zn II ground state to the Zn II resonance state measured by Rogers *et al.*[5] in the near threshold energy region. It is probable because the electron excitation[19] or ionization excitation[20] cross sections of Cd atoms seem to be larger than those of Zn atoms for the similar configuration states. Moreover, the excitation cross sections of the resonance lines of the metallic ions Mg^+,[8] Ba^+,[8–10] Ca^+,[7,8] and Sr^+ (Ref. 8) are of the order of 10^{-15} cm^2 in the near threshold energy region. It is reasonable therefore that $\sigma(5p\,^2P_{3/2})$ is of the order of 10^{-15} cm^2 in the near threshold energy region.

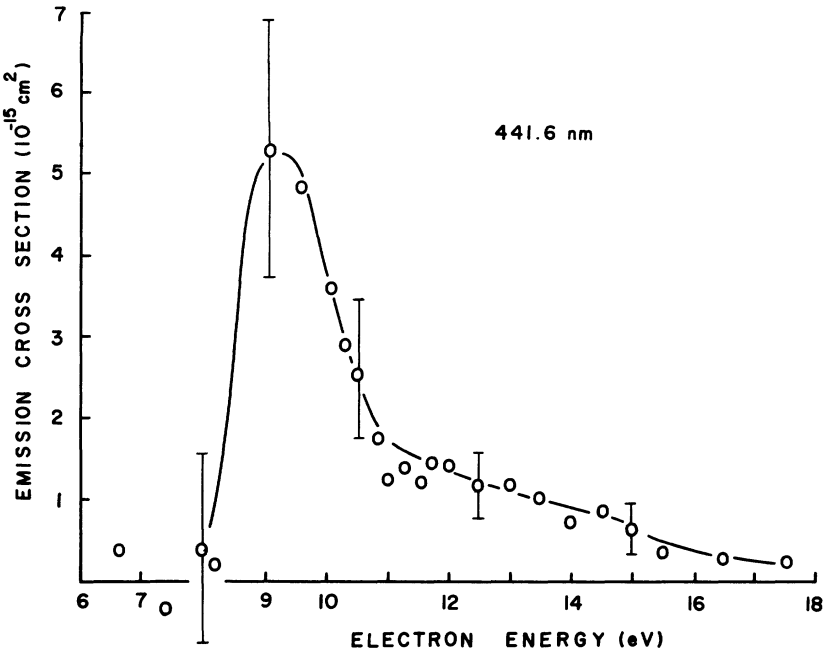

FIG. 6. Absolute emission cross section for the Cd II 441.6-nm line.

B. 441.6-nm line

Figure 6 shows the measured absolute emission cross section of the 441.6-nm line as a function of the electron energy. The uncertainties of the measured emission cross section was evaluated in the same way as described in Sec. III A. The uncertainty of the measured signal count was about ±30%. The uncertainty being caused by the measured ion and electron beam currents and the calibration of the sensitivity of the optical detection system was about ±15%. Combining those uncertainties in quadrature, the total uncertainty was ±35%. The uncertainty was somewhat larger around threshold energy because of small signal count rate.

The influence of the polarization fraction P of the 441.6-nm line on the emission cross section was evaluated to be less than 10% in the electron-energy region measured here. Thus no attempt was made to correct the measured cross section for the polarization fraction.

The measured cross section has a sharp peak around the threshold energy for the excitation and decreases rapidly with the increase of the electron energy. Such sharp peaks at the threshold energy generally appear in the cross sections for the optically forbidden states of Hg,[21] etc. This is similar to the excitation cross sections for the several Beutler states ($4p4s$) of atomic Cu obtained by Aleksakhin *et al.*[22] using the optical method, but is somewhat different from the shape of the cross section for the $4s^2\,^2D_{5/2}$ state of Cu.[23]

According to the study of Cd discharges,[24] all excited states which have prominent cascading lines to the $5s^2\,^2D_{5/2}$ state have higher energies than the $5s^2\,^2D_{5/2}$ state by more than 5 eV. The emission cross section of the 441.6-nm line measured in the range of the threshold energy (8.6 eV) to 14 eV is never influenced by the cascading from the higher states. Above 14 eV, since any appreciable hump is not observed in the measured emission cross section, the influence of the cascading is likely to be negligible. Since the 441.6-nm line is the only spectral line originating from the $5s^2\,^2D_{5/2}$ state, the measured emission cross section of the 441.6-nm line is equal to the absolute excitation cross section of the $5s^2\,^2D_{5/2}$ state [$\sigma(5s^2\,^2D_{5/2})$].

Although the excitation of the inner-shell electron may be less probable than that of an outer-shell electron generally, the determined value of $\sigma(5s^2\,^2D_{5/2})$ is rather large and is of the same order of magnitude as that of $\sigma(5p\,^2P_{3/2})$ at near threshold energies. The relative sensitivity of the optical detection system with wavelength was calibrated carefully as mentioned in Sec. II C. Moreover, the ratio of the emission cross sections of the direct excitations from the Cd ground state to the $5s^2\,^2D_{5/2}$ and $5p\,^2P_{3/2}$ states obtained by using the Cd atom source instead of the Cd^+ ion source without any modification of the optical detection system agreed well with that reported by Vershavskii *et al.*[25] Therefore the measured relative sensitivities at the 441.6- and 214.4-

nm wavelengths seem to be reliable. It is certain that

$$\sigma(5s^2\,{}^2D_{5/2})/\sigma(5p\,{}^2P_{3/2})$$

is close to unity at the electron energy of about 10 eV. Since $\sigma(5p\,{}^2P_{3/2})$ can be of the order of 10^{-15} cm^2 as described in Sec. III A, $\sigma(5s^2\,{}^2D_{5/2})$ is of the order of 10^{-15} cm^2 at the near threshold energy. This is the order of magnitude of the cross section assumed by Mori *et al.* to account for the population density of $5s^2\,{}^2D_{5/2}$ state by the stepwise excitation process. Thus the dominance of the stepwise excitation process for the laser upper state $5s^2\,{}^2D_{5/2}$ has been proved.

ACKNOWLEDGMENTS

The authors are very grateful to Dr. S. Inaba at Gifu Technical College for his useful advice and also to M. Okuda for his assistance in the experiments.

[1]M. Mori, M. Murayama, T. Goto, and S. Hattori, IEEE J. Quantum Electron. 14, 427 (1978).
[2]T. Goto, J. Phys. D 14, 575 (1981).
[3]T. Goto, K. Hane, and S. Hattori, J. Phys. D 14, 587 (1981).
[4]T. Goto, J. Phys. D 15, 421 (1982).
[5]W. T. Rogers, G. H. Dunn, J. O. Olsen, M. Reading, and G. Stefani, Phys. Rev. A 25, 681 (1982).
[6]D. H. Crandall, R. A. Phaneuf, and G. H. Dunn, Phys. Rev. A 11, 1223 (1975).
[7]P. O. Taylor and G. H. Dunn, Phys. Rev. A 8, 2304 (1973).
[8]I. P. Zapesochnyi, V. A. Kel'man, A. I. Imre, A. I. Dashchenko, and F. F. Danch, Zh. Eksp. Teor. Fiz. 69, 1948 (1975) [Sov. Phys.—JETP 42, 989 (1976)].
[9]M. O. Pace and J. W. Hooper, Phys. Rev. A 7, 2033 (1973).
[10]D. H. Crandall, P. O. Taylor, and G. H. Dunn, Phys. Rev. A 10, 141 (1974).
[11]R. A. Phaneuf, P. O. Taylor, and G. H. Dunn, Phys. Rev. A 14, 2021 (1976).
[12]K. Hane, T. Goto, and S. Hattori, J. Phys. D 15, L47 (1982).
[13]M. Khan and J. M. Schroeer, Rev. Sci. Instrum. 42, 1348 (1971).
[14]A. N. Tripathi, K. C. Mathur, and S. K. Joshi, J. Phys. B 2, 878 (1969).
[15]R. Abouaf, J. Phys. (Paris) 31, 277 (1970).
[16]D. A. Shaw, A. Adams, and G. C. King, J. Phys. B 8, 2456 (1975).
[17]R. Mewe, Astron. Astrophys. 20, 215 (1972).
[18]T. Andersen and G. Sorensen, J. Quant. Spectrosc. Radiat. Transfer 13, 369 (1973).
[19]V. N. Savchenko, Opt. Spektrosk. 30, 12 (1971) [Opt. Spectrosc. (USSR) 30, 6 (1971)].
[20]N. P. Penkin, A. A. Mityureva, and E. R. Zhezherina, Opt. Spektrosk. 33, 1028 (1972) [Opt. Spectrosc. (USSR) 33, 567 (1972)].
[21]R. J. Anderson, E. T. P. Lee, and C. C. Lin, Phys. Rev. 157, 31 (1967).
[22]I. S. Aleksakhin, A. A. Borovik, V. P. Starodub, and I. I. Shafranjosh, Zh. Prikl. Spektrosk. 30, 236 (1979) [J. Appl. Spectrosc. (USSR) 30, 158 (1979)].
[23]S. Trajmar, W. Williams, and S. K. Srivastava, J. Phys. B 10, 3323 (1977).
[24]A. G. Shenstone and J. T. Pittenger, J. Opt. Soc. Am. 39, 219 (1949).
[25]S. P. Varshavskii, A. A. Mityureva, and N. P. Penkin, Opt. Spektrosk. 29, 637 (1970) [Opt. Spectrosc. (USSR) 29, 341 (1970)].